



## Adaptive planning using megavoltage fan-beam CT for radiation therapy with testicular shielding

Poonam Yadav, M.Sc.,<sup>\*†‡</sup> Kevin Kozak, M.D., Ph.D.,<sup>\*</sup> Ranjini Tolakanahalli, M.S.,<sup>\*†</sup>  
V. Ramasubramanian, Ph.D.,<sup>‡</sup> Bhudatt R. Paliwal, Ph.D.,<sup>\*†§</sup> James S. Welsh, M.D., M.S.,<sup>\*†</sup> and Yi Rong, Ph.D.<sup>\*§</sup>

<sup>\*</sup>Department of Human Oncology and <sup>†</sup>Department of Medical Physics, University of Wisconsin, Madison, Madison, WI; <sup>‡</sup>School of Advance Sciences, Vellore Institute of Technology University, Vellore, Tamil Nadu, India; and <sup>§</sup>University of Wisconsin, Riverview Cancer Centre, Wisconsin Rapids, WI

### ARTICLE INFO

#### Article history:

Received 3 January 2011

Accepted 10 June 2011

#### Keywords:

Testicular shielding  
Megavoltage CT imaging  
Dose verification  
Adaptive radiotherapy

### ABSTRACT

This study highlights the use of adaptive planning to accommodate testicular shielding in helical tomotherapy for malignancies of the proximal thigh. Two cases of young men with large soft tissue sarcomas of the proximal thigh are presented. After multidisciplinary evaluation, preoperative radiation therapy was recommended. Both patients were referred for sperm banking and lead shields were used to minimize testicular dose during radiation therapy. To minimize imaging artifacts, kilovoltage CT (kVCT) treatment planning was conducted without shielding. Generous hypothetical contours were generated on each “planning scan” to estimate the location of the lead shield and generate a directionally blocked helical tomotherapy plan. To ensure the accuracy of each plan, megavoltage fan-beam CT (MVCT) scans were obtained at the first treatment and adaptive planning was performed to account for lead shield placement. Two important regions of interest in these cases were femurs and femoral heads. During adaptive planning for the first patient, it was observed that the virtual lead shield contour on kVCT planning images was significantly larger than the actual lead shield used for treatment. However, for the second patient, it was noted that the size of the virtual lead shield contoured on the kVCT image was significantly smaller than the actual shield size. Thus, new adaptive plans based on MVCT images were generated and used for treatment. The planning target volume was underdosed up to 2% and had higher maximum doses without adaptive planning. In conclusion, the treatment of the upper thigh, particularly in young men, presents several clinical challenges, including preservation of gonadal function. In such circumstances, adaptive planning using MVCT can ensure accurate dose delivery even in the presence of high-density testicular shields.

Published by Elsevier Inc. on behalf of American Association of Medical Dosimetrists.

### Introduction

An ideal radiotherapy plan should deliver optimum dose to the target volume while sparing the adjacent critical nontarget tissues. Normal and tumor tissues have a wide spectrum of radio-sensitivities. Normal tissue tolerance doses vary with the type and volume of tissue irradiated, radiation quality, radiation schedule, and the tolerance endpoint. Consequently, unique strategies for radioprotection have been developed to preserve normal tissue function.<sup>1–4</sup> Testes are among the most sensitive normal tissues. To preserve gonadal function, several strategies including sperm banking, dose de-escalation, modifications of radiated volume, and testicular shielding can be applied. For diagnostic studies, Hohl and col-

leagues have shown that 1 mm of lead gonadal shielding reduces testicular dose from a multi-detector computed tomography (CT) scan by 87%.<sup>5</sup> The estimated thresholds for temporary as well as permanent sterility in man are 0.15 and 3.5–6 Sv, respectively, for single brief exposure, and are paradoxically even lower when the dose is fractionated as a result of reassortment through the cell cycle of the exquisitely radiosensitive spermatogonia.<sup>6</sup> In addition to sterility, scattered radiation to the testes may increase risks of genetic abnormality in the offspring of the irradiated patient. Higher radiation doses may also lead to endocrine dysfunction and testicular atrophy.<sup>7–9</sup>

Measurements of testicular dose have been done with and without shielding materials using thermoluminescent dosimeters, ion chamber, and diodes.<sup>10</sup> Bieri and colleagues demonstrated that testicular shielding reduced testicular doses from 3.89 to 1.48 cGy per fraction when para-aortic and homolateral iliac lymph nodes were treated, and from 1.86 to 0.65 cGy per fraction when only para-

Dr. Rong has received travel sponsorship from TomoTherapy, Inc. James S. Welsh has received honoraria for speaking for TomoTherapy, Inc.

Reprint requests to: Yi Rong, Ph.D., 410 Dewey Street, Wisconsin Rapids, WI 54494.

E-mail: [rong@humonc.wisc.edu](mailto:rong@humonc.wisc.edu)

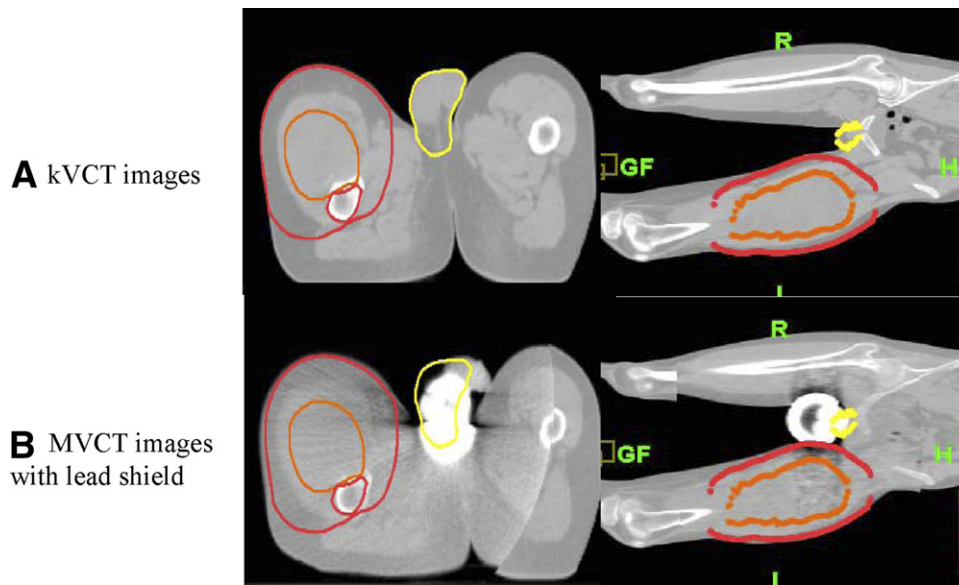


Fig. 1. (A) kVCT images; (B) MVCT images with lead shield.

aortic lymph nodes were treated in early-stage seminoma patients.<sup>11</sup> Also, when radiation target volumes are more proximal to the testes, the absolute dose reduction conferred by lead shielding is anticipated to be even greater. Code of Federal Regulations (CFR) 21, specifically in reference to medical diagnostic radiographic procedures, recommends that gonadal shielding be provided when the gonads lie within the primary radiographic field, or within close proximity (about 5 cm), despite proper beam limitation. CFR 21 also recommends that gonad shielding provide attenuation of x-rays at least equivalent to that afforded by 0.25 mm of lead.<sup>12</sup>

The use of kilovoltage CT (kVCT) for radiation planning is impractical with a testicular lead shield because there is data inconsistency caused by photon starvation because the presence of metal produces severe streaks in the reconstructed CT slices. However, the image quality of MVCT (megavoltage CT) is acceptable for planning, and an MVCT offers considerably reduced artifact for patients with metal implants.<sup>13-15</sup> We examined adaptive planning with MVCT imaging for 2

young male patients with proximal thigh lesions and testicular shielding that was used during treatment. Helical tomotherapy (TomoTherapy Hi-Art Unit, TomoTherapy, Inc., Madison, WI) was used for treatment delivery. Results were compared with kVCT-derived radiotherapy plans.

#### Materials and Methods

##### Patient history and diagnosis

Both patients were 19-year-old males. One patient (patient A) had a high-grade, malignant peripheral nerve sheath tumor of the proximal left thigh measuring  $11 \times 6 \times 6$  cm<sup>3</sup>. The other patient (patient B) had a high-grade, pleomorphic sarcoma, not otherwise specified, of the proximal left thigh measuring  $21 \times 12 \times 11$  cm<sup>3</sup>. At presentation, neither patient had demonstrable distant metastatic disease.

##### Treatment setup and planning

After multidisciplinary evaluation, both patients were treated with image-guided, neoadjuvant radiation therapy using helical tomotherapy. Patient A was

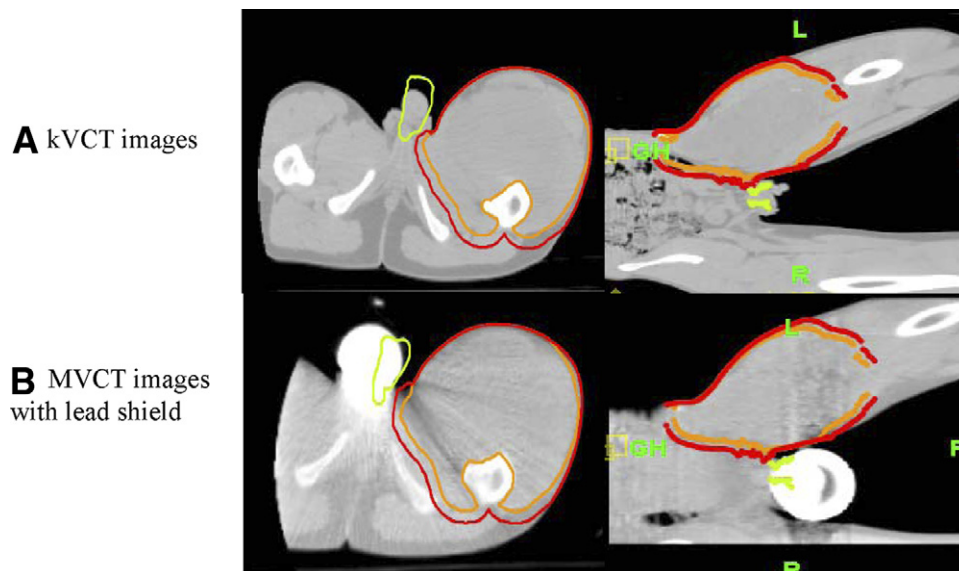


Fig. 2. (A) kVCT images; (B) MVCT images with lead shield.

**Table 1**

Parameters—pitch, modulation factor, field width, treatment time, and gantry period used to generate tomotherapy plans for both patients

	Patient A	Patient B
PTV length (cm)	23	21
Pitch	0.430	0.430
Field width (cm)	5.0	2.5
Modulation factor (actual)	1.8 (1.710)	2.4 (2.395)
Treatment duration (s)	251.5	836.5
Gantry period (s)	15	30

treated to a dose of 24 Gy delivered in 20 hyperfractionated sessions (1.2 Gy twice daily). Patient B was initially planned to receive a total dose of 50.4 Gy in 28, 1.8-Gy daily fractions. However, serial clinical examination during treatment revealed significant tumor softening and modest tumor shrinkage and the radiation course was truncated at a total dose of 45 Gy to reduce the probability of late toxicity. The dosimetric goal was to achieve the prescribed dose for 95% of the planning target volume (PTV).

Both patients were originally scanned without a lead shield using a diagnostic CT scanner. The kVCT images were used to generate initial treatment plans. kVCT images were exported to the Pinnacle planning Station (version 8.0 m, Philips Radiation Oncology Systems, Madison, WI) for observing the target volume and normal tissue segmentation. In addition to femoral heads, femurs, bladder, rectum, anus, and target volumes, a virtual contour surrounding the testes was delineated on the kVCT images for directional blocking of the primary beam. For patient A, the delineated virtual contour followed the shape of the testes (Fig. 1). For patient B, a rectangular contour was drawn surrounding the testes with a much larger volume to estimate the actual lead shield size (Fig. 2). The contour of the right thigh was set to directional block for both patients. Finally, contours and images were exported to the TomoTherapy planning station. Table 1 shows the planning parameters, namely pitch, modulation factor, field width, and gantry period.

*Dose verification and plan adaptive*

TomoTherapy plans are based on intensity modulation necessitating delivery quality assurance (DQA) before treatment. DQA plans were generated on the planning station and delivered using a TomoTherapy “cheese” phantom with the ion-chamber/film system. The pretreatment measurement shows that the measured dose using an ion chamber/film for both patients was within ± 3%/3 mm of the expected dose, thus meeting quality assurance requirements.

Pretreatment MVCT imaging was used for position verification in both cases. Figures 1 and 2 show the diagnostic kVCT images without lead shielding at initial simulation and MVCT images acquired on the first day of the treatment using 3.5-MV photon beam energy and 40 × 40-cm<sup>2</sup> field of view in normal (slice thickness: 4 mm) mode. Apart from the use of laser alignment, acquiring daily MVCT images is the clinical protocol for patient alignment. It also can be further used for image-guided adaptive radiotherapy, which covers a large scope of other techniques, including dose reconstruction,<sup>16</sup> dose accumulation,<sup>17</sup> treatment evaluation,<sup>18</sup> recontouring and reoptimization.<sup>19,20</sup> Using the MVCT image set acquired on the first day of treatment and delivered kVCT plan sinogram, verification doses were calculated using the TomoTherapy planned Adaptive application for both patients to analyze the accuracy of delivered dose and the effect of testicular shielding. For generating the adaptive plan, the density of the streaking artifacts generated from the testicular shielding on patients were overridden to 1. Contours, including the PTV and femoral heads, were modified on the new MVCT datasets, which were then used for the generation of adaptive plans. A new DQA plan was generated for the adaptive plan using TomoTherapy “cheese” phantom with the ion-chamber/film system. The DQA plan passed meeting the quality assurance requirements.

**Results**

Artifacts caused by the lead shielding are evidenced on MVCT images (Figs 1 and 2), although these artifacts are much less significant compared with kVCT imaging.<sup>5</sup> Contours of the testes and

**Table 2**

PTV receiving 90%, 95%, 100%, and 110% of the prescribed dose (24 Gy) in kVCT plan, verification plan, and adaptive plan for patient A

	kVCT plan	Verification plan	Adaptive plan
90% of prescribed dose	99.76%	98.92%	99.72%
95% of prescribed dose	99.15%	97.21%	99.31%
100% of prescribed dose	99.75%	97.89%	99.54%
110% of prescribed dose	0.845%	1.93%	0%

**Table 3**

PTV receiving 90%, 95%, 100%, and 110% of the prescribed dose (50.4 Gy) in kVCT plan, verification plan, and adaptive plan for patient B

	kVCT plan	Verification plan	Adaptive plan
90% of prescribed dose	99.99%	99.75%	99.91%
95% of prescribed dose	99.96%	99.47%	99.56%
100% of prescribed dose	97.03%	96.78%	96.98%
110% of prescribed dose	0.013%	0.61%	0.46%

right thigh were sufficient to block most of the beams incident from the right side for both patients. PTVs receiving 110%, 100%, 95%, and 90% of the prescribed dose are shown in Tables 2 and 3 for patients A and B, respectively, for all 3 plans (kVCT, verification, and MVCT plans). Adequate thigh separation resulted in superior shield placement, as is evident in the case of patient B (Fig. 2) compared with patient A, who had insufficient thigh separation (Fig. 1). This led to deformation of the PTV in patient A, particularly around the testic-

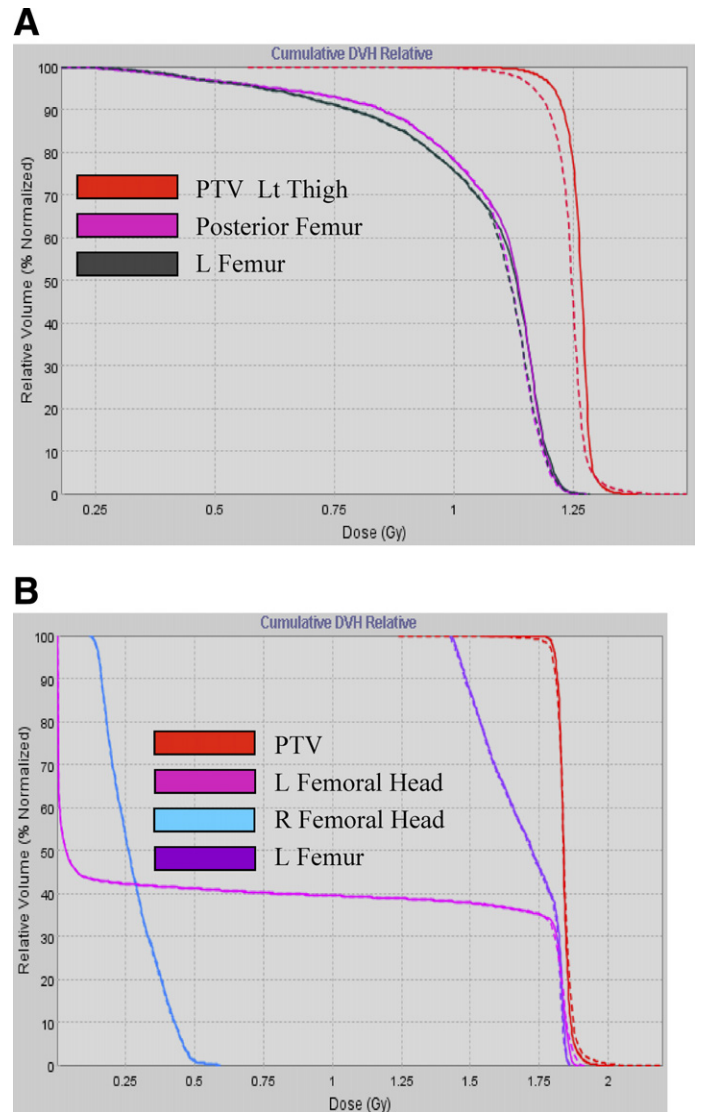


**Fig. 3.** (A) Dose volume histogram (DVH) comparison of planned dose (on kVCT image, solid lines) and verification dose (on MVCT image, dashed lines) for patient A. PTV left thigh, posterior femur and left femur are represented on DVH. (B) Dose volume histogram (DVH) comparison of planned dose (on kVCT image solid lines) and verification dose (dashed lines on MVCT image) for patient B. PTV, left and right femur head and left femur are represented on DVH.

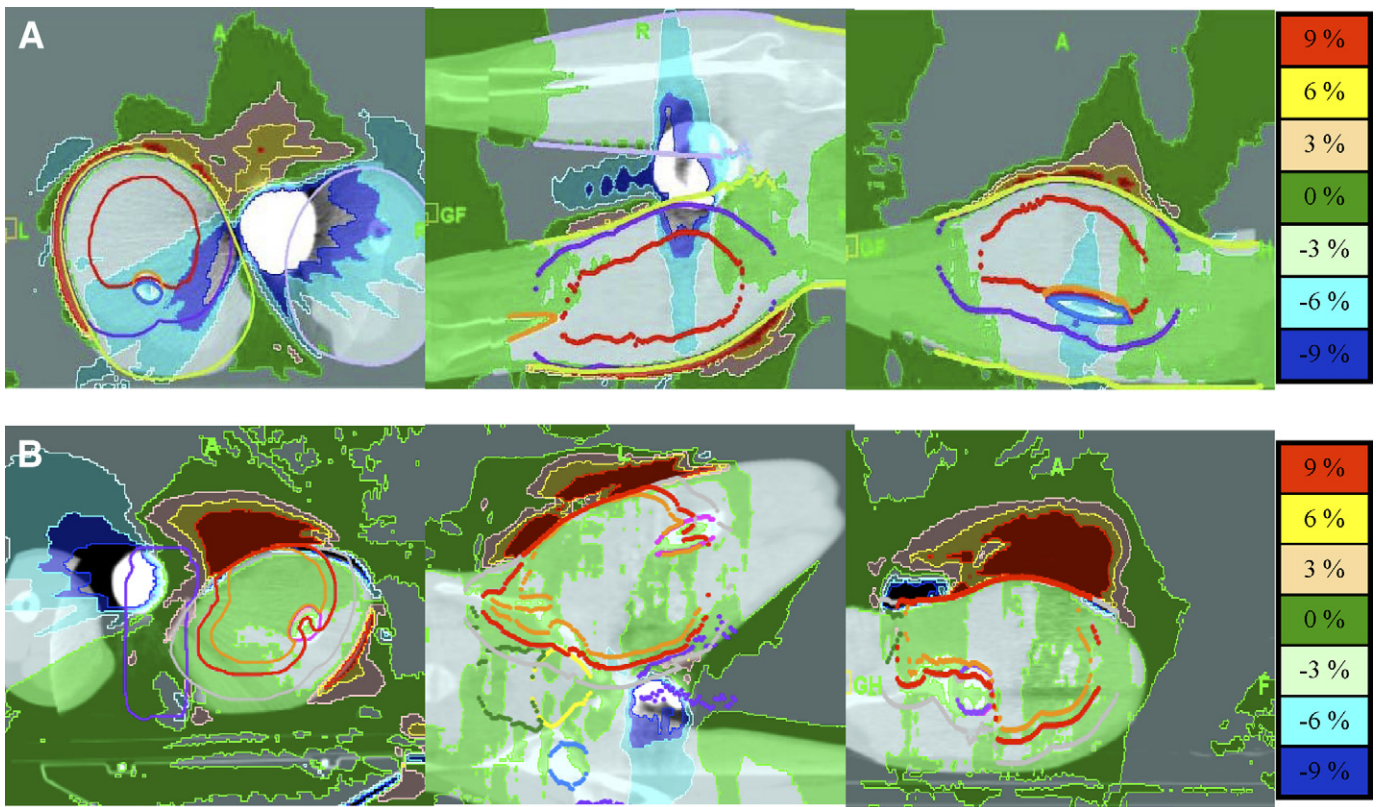


Fig. 4. Isodose lines showing  $\pm 9\%$ ,  $\pm 6\%$ ,  $\pm 3\%$  and zero dose difference between planned and verification dose for (A) patient A and (B) patient B.

ular shield. As a result, 2% underdosing was observed in the verification plan when compared with the original plan for patient A. This difference was  $<1\%$  for patient B. The differences in dose-volume histograms (DVHs) for verification and adaptive plans are shown in Fig. 3. Dose-difference isodose lines between the original and verification plans for 0%,  $\pm 3\%$ ,  $\pm 6\%$ , and  $\pm 9\%$  are shown in Fig. 4. Differences higher than 5% are primarily located in the lead shield area and the downstream area of the beams for patients A and B, as well as the target volume that abuts the lead shield in

patient A. Adaptive plans were generated for both patients to receive more accurate dose delivery with modified target delineation using the same optimization parameters. Same, if not better, plan quality and dose distribution were achieved for adaptive plans compared with the original kVCT plans. Significant difference in dose to posterior femur and left femur for patient A on DVHs (Fig. 5) are observed between adaptive and verification plan for the entire treatment. This difference is negligible for patient B (Fig. 6) because of minimum deformation in PTV.

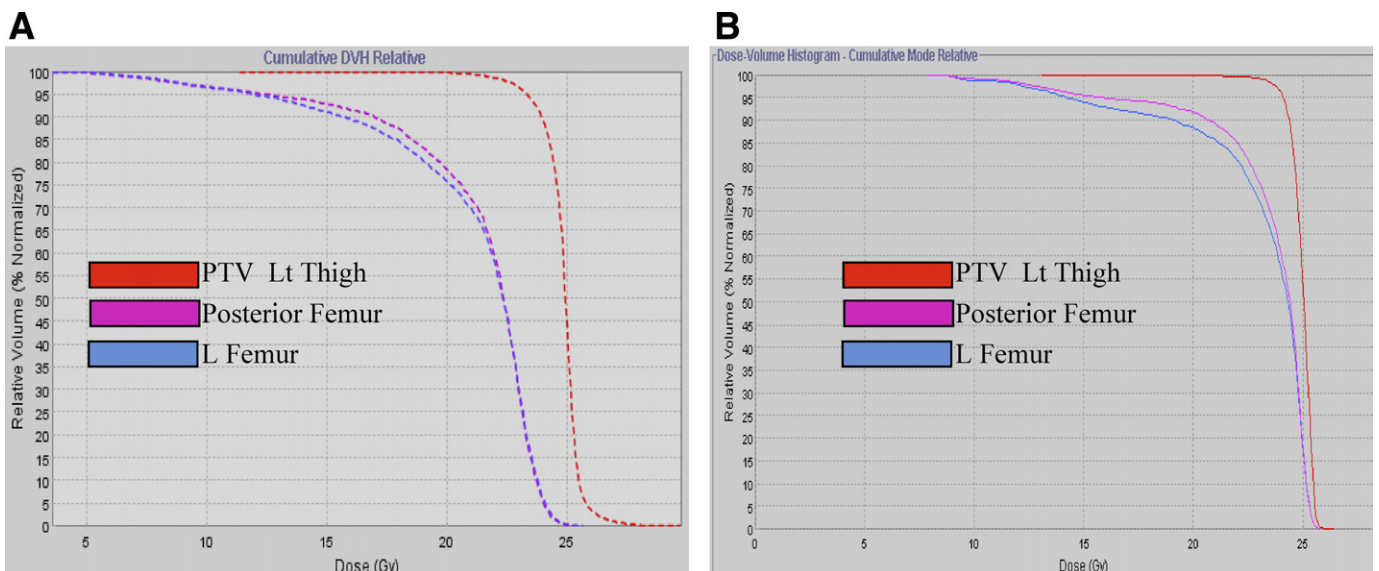


Fig. 5. DVH from total treatment (A) verification and (B) adaptive plan for patient A. PTV left thigh, posterior femur and left femur respectively are presented on DVH's.

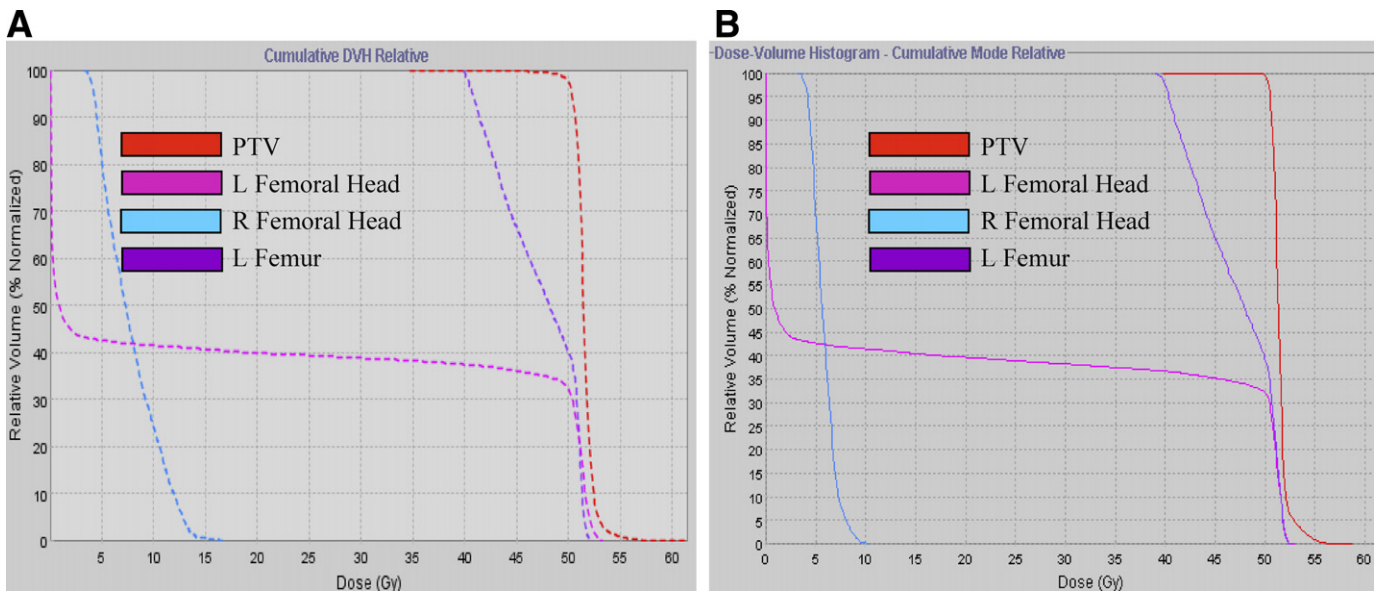


Fig. 6. DVH from total treatment (A) verification and (B) adaptive plan for patient B. PTV left thigh, posterior femur and left femur respectively are presented on DVH's.

## Discussion and conclusion

Niroomand-rad *et al.* discussed the concept of “significant dose” emphasizing the risk of genetic abnormalities.<sup>21</sup> Gonadal shielding was recommended for male patients to reduce the genetic risk to subsequent generations to negligible levels. The gonadal shield allows a 3- to 10-fold reduction in dose to the testes, depending primarily on the distance from the edge of the target volume to the gonads. When the shield is used, the dose is generally <1% of the patient's prescription dose.<sup>22</sup> Testicular shields are high attenuation materials, and consideration of their impact on dose delivery during treatment planning is indispensable for accurate dose calculation. In this study, a method is described to accommodate testicular shielding using adaptive planning with MVCT for young male patients undergoing helical tomotherapy for target volumes located near the gonads. Helical delivery with TomoTherapy uses multiple beam angles over 360 degrees to optimize conformity. In this study, beams were prevented from entering through the lead shields and the contralateral thigh to minimize dose to the genital area and prevent shield attenuation of treatment beams. Inaccurate delineation of the blocking can lead to 2 errors. First, underestimation of the region requiring directional blocking can result in beam entry through contralateral thigh or gonadal shield, resulting in target volume underdosing. In contrast, overestimation of the region requiring directional blocking limits entry angles and may reduce plan conformality. Inaccuracies in the exact shape and position of the virtual shield, which is delineated on kVCT images, are also possible. However, the exact size, shape, and position of the actual lead shield cannot be accurately ascertained on kVCT images if the shield were in place during the image acquisition because of artifact. Thus, directional blocks are based on virtual shields created on the kVCT images during treatment planning. As described, MVCT scans, taken with real shielding in place, can be used for adaptive planning and more refined directional blocking. It has been observed that compared with kVCT, MVCT images exhibit considerably reduced artifacts in metal implants, such as hip implants, surgical clips, and dental fillings, and provide good agreement to measurements in dose prediction.<sup>23, 24</sup> The “Planned Adaptive Program” in the TomoTherapy Planning Station provides a clinical tool to accommodate alterations in patient setup (*i.e.*, the addition of a gonadal shield) and provides dosimetry verification

and modification using pretreatment MVCT images. It is worth noting that although metal artifacts in MVCT images are dramatically less significant compared with the kVCT images, they are not completely eliminated, as shown in the presented cases (Figs. 1 and 2). In the case of patient A, there is underdosing in the target area because insufficient thigh separation led to PTV deformation. We suggest that for such cases, adequate distance should separate the thighs during kV imaging. Also we recommend a density override to a value of 1 before the adaptive planning procedure, even when using MVCT images. Otherwise an underdosing in the target area will be observed because the CT numbers in the area of close proximity to the gonadal shield will be underestimated because of metal artifacts induced from the significant photon attenuation from the high-density materials. A large shielding device to the testes is afforded by abducting the thigh from the midline, out of the radiation field. Daily pretreatment MVCT scans allow precise patient positioning and ensure fidelity of the shield. To avoid artifacts caused by the high-density clamshell shield, one option is to use low-density material, such as a wooden clamshell shield, to estimate virtual contours for beam blocking. The geometry of the wooden clamshells used for simulation should be identical to the lead shielding used for treatment. This simple setup allows for accurate directional blocks and will minimize daily setup variation. This will also ensure adequate abduction of the legs for insertion of the clamshells.

In the absence of alternative techniques, such as low-density clamshell for simulating the lead shield, these cases demonstrated the feasibility of using MVCT images with adaptive planning to accurately accommodate testicle shielding, verify patient positioning, and ensure accurate target volume and normal tissue dosimetry.

## References

1. Antolak, J.A., Strom, E.A. Fetal dose estimates for electron-beam treatment to the chest wall of a pregnant patient. *Med. Phys.* **25**:2388–91; 1998.
2. Hayashi, K.; Hatsuno, K.; Yoshimura, R.; *et al.* Electron Therapy for Orbital and Periorbital Lesions Using Customized lead Eye Shields. *Ophthalmologica.* **223**:96–101; 2009.
3. Brnić, Z.; Vekić, B.; Hebrang, A.; *et al.* Efficacy of breast shielding during CT of the head. *Eur. Radiol.* **13**:2436–40; 2003.
4. Beaconsfield, T.; Nicholson, R.; Thornton, A.; *et al.* Would thyroid and breast shielding be beneficial in CT of the head? *Eur. Radiol.* **8**:664–7; 1998.

5. Hohl, C.; Mahnken, A.H.; Klotz, E.; *et al.* Radiation dose reduction to the male gonads during MDCT: The effectiveness of a lead shield. *AJR Am. J. Roentgenol.* **184**:128–30; 2005.
6. ICRP. The 2007 Recommendations of the International Commission on Radiological Protection. ICRP publication 103. *Ann. ICRP.* **37**:1–332; 2007.
7. Jacobsen, K.D.; Olsen, D.R.; Fossa, K.; Fossa, S.D. External beam abdominal radiotherapy in patients with seminoma stage I: Field type, testicular dose and spermatogenesis. *Int. J. Radiat. Oncol. Biol. Phys.* **38**:95–102; 1997.
8. Boehmer, D.; Badakhshi, H.; Kuschke, W.; *et al.* Testicular dose in prostate cancer radiotherapy: Impact on impairment of fertility and hormonal function. *Strahlenther. Onkol.* **181**:179–84; 2005.
9. Daniell, H.W.; Tam, E.W. Testicular atrophy in therapeutic orchiectomy specimens from men with prostate carcinoma: Association with prior prostate bed radiation and older age. *Cancer* **83**:1174–9; 1998.
10. Nazmy, M.S.; El-Taher, M.M.; Attalla, E.M.; *et al.* Shielding for Scattered Radiation to the Testis during Pelvic Radiotherapy: Is it worth? *J. Egypt. Natl Cancer Inst.* **19**:127–32; 2007.
11. Bierri, S.; Rouzaud, M.; Mirabell, R. Seminoma of the testis: Is scrotal shielding necessary when radiotherapy is limited to the para-aortic nodes? *Radiother. Oncol.* **50**:349–53; 1999.
12. Bobka, M.S. The 21 CFR (Code of Federal Regulations) online database: Food and Drug Administration regulations full-text. *Med. Ref. Serv. Q.* **12**:7–15; 1993.
13. Schreiner, L.J.; Roger, M.; Salomons, G.J.; *et al.* Metal artifacts suppression megavoltage computed tomography. *J. Med. Imaging* **5745**:637–45; 2005.
14. Hong, T.S.; Welsh, J.S.; Ritter, M.A.; *et al.* Megavoltage computed tomography: An emerging tool for image-guided radiotherapy. *Am. J. Clin. Oncol.* **30**:617–23; 2007.
15. Rong, Y.; Fahner, T.; Welsh, J.S. Hypofractionated Breast and Chest Wall Irradiation using Simultaneous In-field Boost IMRT Delivered via Helical Tomotherapy. *Technol. Cancer Res. Treat.* **7**:433–40; 2008.
16. Kapatoes, J.M.; Olivera, G.H.; Balog, J.P.; *et al.* On the accuracy and effectiveness of dose reconstruction for tomotherapy. *Phys. Med. Biol.* **46**:943–66; 2001.
17. Yan, D.; Vicini, F.; Wong, J.; *et al.* Adaptive radiation therapy. *Phys. Med. Biol.* **42**:123–32; 1997.
18. Vargas, C.; Martinez, A.; Kestin, L.L.; *et al.* Dose-volume analysis of predictors for chronic rectal toxicity after treatment of prostate cancer with adaptive image-guided radiotherapy. *Int. J. Radiat. Oncol. Biol. Phys.* **62**:1297–308; 2005.
19. Lu, W.; Olivera, G.H.; Chen, Q.; *et al.* Deformable registration of the planning image (kVCT) and the daily images (MVCT) for adaptive radiation therapy. *Phys. Med. Biol.* **51**:4357–74; 2006.
20. Wu, C.; Jeraj, R.; Olivera, G.H.; *et al.* Re-optimization in adaptive radiotherapy. *Phys. Med. Biol.* **47**:3181–95; 2002.
21. Niroomand-Rad, A.; Cumberlin, R. Measured dose to ovaries and testes from Hodgkin's fields and determination of genetically significant dose. *Int. J. Radiat. Oncol. Biol. Phys.* **25**:745–51; 1993.
22. Fraass, B.A.; Kinseela, T.J.; Harrington, F.S.; *et al.* Peripheral dose to the testes: The design and clinical use of a practical and effective gonad shield. *Int. J. Radiat. Oncol. Biol. Phys.* **11**:609–15; 1985.
23. Yang, C.; Liu, T.; Jennelle, R.L.; *et al.* Utility of megavoltage fan-beam CT for treatment planning in a head-and-neck cancer patient with extensive dental fillings undergoing helical tomotherapy. *Med. Dosim.* **35**:108–14; 2010.
24. Meeks, S.; Langen, K.; Wagner, T.; *et al.* The use of MVCT images for dose calculation in the presence of metallic objects. *Med. Phys.* **32**:2115; 2005.